IEEE Access
Multidisciplinary | Rapid Review | Open Access Journal

Received May 22, 2021, accepted July 13, 2021, date of publication July 19, 2021, date of current version July 28, 2021.

Digital Object Identifier 10.1109/ACCESS.2021.3098042

Ferromagnetic Silicene Superlattice Based Thermoelectric Flexible Renewable Energy Generator Device

MOHAMMED M. EL-BANNA[1], ADEL HELMY PHILLIPS[1], AND AHMED SAEED ABDELRAZEK BAYOUMI[2]

[1]Department of Engineering Physics and Mathematics, Faculty of Engineering, Ain Shams University, Cairo 11517, Egypt
[2]Department of Engineering Physics and Mathematics, Faculty of Engineering, Kafrelsheikh University, Kafrelsheikh 33516, Egypt

Corresponding author: Mohammed M. El-Banna (mm.elbanna@eng.asu.edu.eg)

ABSTRACT The object of the current research manuscript is to analyze the valley-spin thermoelectric properties and Nernst coefficient at two different temperatures for ferromagnetic silicene superlattice. Photon-assisted tunneling probability is used to identify the resolved thermoelectric parameters including (valley, spin, and charge) electronic thermal conductance, Seebeck coefficient, figure of merit, and also electrical conductance and Nernst coefficient. The results show oscillatory behavior to all investigated parameters. The improved data of Seebeck coefficient (valley, spin, and charge) could be because of quantum confinement effect of the present investigated nanodevice. The figure of merit (valley, spin, and charge) attains quite high values with good high thermoelectric efficiency. The enhancement of Nernst coefficient (valley, spin, and charge) might consider Nernst effect is suitable for thermoelectric heat energy conversion system of the present flexible ferromagnetic silicene superlattice. The ferromagnetic silicene superlattice nanodevices are good candidates for flexible renewable energy generation as demonstrated by this analysis.

INDEX TERMS Electron thermal conductance, Seebeck coefficient, electrical conductance, figure of merit, thermoelectric efficiency, Nernst coefficient.

I. INTRODUCTION

The dramatic increase of power demand in electrical power grids is noticed in the recent decades. Added to that, the environmental concerns and economic constrains initiate many research efforts in different aspects. Many efforts are investigated for involving the different types of renewable energy resources into electrical grid for enhancing the overall system performance as for solving the optimal power flow [1], modeling of solar cells and modules [2]for improving the efficiency of radial distribution systems with wind power existence [3], [4], for economic and environmental concerns [5], for considering the economic concerns in emergency events [6], and for solving reactive power problem with renewable energy resources [7]. The need of flexible renewable energy generation acts an important issue to assure acceptable performance of renewable energy resources. So, the motivation of this work lies in this trend.

The associate editor coordinating the review of this manuscript and approving it for publication was Yee Sin Ang.

On the other hand, around half of the world's generated energy is wasted as heat [8]–[11]. The electricity generation from the temperature gradient using thermoelectric, solid-state devices could be a good waste heat energy recovery [8]–[11]. Heat produced by unconcentrated or concentrated sunlight can also be converted to electrical power using thermoelectric devices. The importance here comes from the fact that the radiation in infrared range has photon energy lower than the photo-sensitizers band gap so it is squandered as heat [8]–[11]. Without moving parts, the Peltier effect and Seebeck effect can directly convert heat to electricity so that, thermoelectric materials can handle a lot of energy problems. The efficiency of thermoelectric conversion can be measured by the dimensionless figure of merit [12]–[16]. In spintronics and conventional electronics to process and carry information the two intrinsic electron characteristics, spin and charge are utilized [17]–[19]. Recently, there is another degree of freedom in some materials, the valley degree of freedom, which can be utilized to process and carry information, and this research field is called valleytronics [20]–[23]. Many literatures in this field emphasis the ability of superlattice

structures to successfully control the transport properties of graphene [24], [25], silicene [26], [27] and semiconductors [28], [29].

The phenomena of thermoelectric and spin transport involving spin Seebeck tunneling [30], anomalous Nernst effects [31], [32], spin [32], thermal spin transfer torque [33], and spin dependent thermopower [34] are related in the spin caloritronics field. In monolayer transition metal dichalcogenides (TMDCs), theoretically, various valley/spin -dependent thermoelectric effects already have been anticipated, involving valley Nernst effect (VNE) [35]–[37] and spin Nernst effect, which is the thermoelectric analogy of the spin Hall effect [38], [39].

Therefore, a new field has been aroused called valley caloritronics in [40]–[42]as the experimental demonstration of these effects with help of spin-valley degree of freedom, which is more reliable than spin regarded to external magnetic fields because of enormous intrinsic spin–orbit coupling (SOC).

Non-volatility, ultra-low heat dissipation and faster speed make spintronic devices a perfect candidate for electronics' future. In addition, because of their remarkable spin-dependent properties, such as spin diffusion length, Rashba SOC, ultra-long spin relaxation time, quantum spin Hall effect and spin-valley locking, 2D materials such as black phosphorus (BP), graphene, silicene [43] and TMDCs have provided an excellent forum for spintronic study.

Additionally, new opportunities for the practical application of spintronics have been brought by 2D materials, and improvements are expected in low-power computing, communication and storage. For nanoelectronic applications, silicene, a cousin of graphene, is presently of interest to studies in the area of 2D materials [40], [41], [44]. Compared to graphene and other 2D materials, the benefits of silicene are that it is compatible with existing silicon-based electronics and can easily be integrated into them [42].

It is well known that the effect of both Nernst coefficient and valley degree of freedom on spin thermoelectric energy efficiency has not been considered upto this moment in ferromagnetic silicene superlattice. So, this work aims to explore thermoelectric energy conversion and valley-spin Nernst effect of ferromagnetic silicene superlattice. The important features can be summarized as:

- The valley-spin thermoelectric properties and Nernst coefficient at two different temperatures for ferromagnetic silicene superlattice are investigated.
- The oscillatory behavior of all parameters is discussed.
- The figure of merits (valley, spin, and charge) attains quite high values at good high thermoelectric efficiency.
- The enhancement of Nernst coefficient (valley, spin, and charge) considering the Nernst effect is suitable for thermoelectric heat energy conversion system of the presented flexible ferromagnetic silicene superlattice.
- The ferromagnetic silicene superlattice nanodevices can be considered as good candidates for flexible renewable energy generation.

II. THE PROPOSED DEVICE

2N ferromagnetic strips interweave (2N-1) normal strips of equally length single-layer silicene [27], [45] are forming the proposed model. This device's source and drain are formed of metal as seen in Fig. 1.

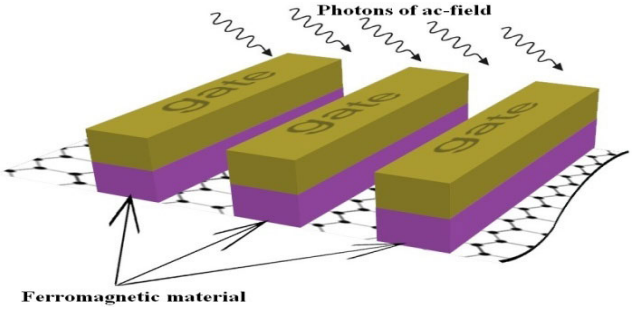

FIGURE 1. A schematic diagram of the proposed model.

The transport of valley-spin polarization under induced ac field is implemented. Photon-assisted conduction channels also can be introduced with help of ac-oscillating fields which can be modulated with the gated voltage to set it into the window of conduction of the device [23], [27], [45]–[47]. The transport is distinguishable for spin alignment because of Zeeman splitting which is imposed in presence of magnetic field, there are valley possibilities also in addition to conduction channels of the photo-assisted transport, so this resulted in photon-assisted spin and valley resolved conduction. The tunneling probability, $\Gamma_{\text{ac-field(E)}}$, is calculated as [27], [45]:

$$\Gamma_{ac-field}(E) = \sum_{n=1}^{\infty} J_n^2\left(\frac{eV_{ac}}{n\hbar\omega}\right).\left|t_{\eta\sigma}\right|^2 \tag{1}$$

where $J_n\left(\frac{eV_{ac}}{n\hbar\omega}\right)$ is first kind Bessel function of order n^{th}, V_{ac} is the induced ac-field peak and ω is its angular frequency and $t\eta\sigma$ represents transmission coefficient, with $\eta(\eta') = +1(-1)$ conforms to $K(K')$ valley, $\sigma = +1(-1)$ is for up spin and down spin configuration [27], [45].

The categories of conductance, G, in silicene are [48]–[50]:
Valley resolved conductance, $G_{K(K')}$, is:

$$G_{K(K')} = \frac{G_{K(K')\uparrow\uparrow} + G_{K(K')\uparrow\downarrow}}{2} \tag{2}$$

The spin alignments are distinguished by $\uparrow\uparrow$ for parallel and $\uparrow\downarrow$ for antiparallel. Spin resolved conductance, $G_{\uparrow\uparrow(\uparrow\downarrow)}$ is:

$$G_{\uparrow\uparrow(\uparrow\downarrow)} = \frac{G_{K\uparrow\uparrow(\uparrow\downarrow)} + G_{K'\uparrow\uparrow(\uparrow\downarrow)}}{2} \tag{3}$$

The Dirac fermion conductance for the three cases charge, valley and spin respectively are:

$$G_C = \frac{1}{2}(G_{\uparrow\uparrow} + G_{\uparrow\downarrow}) \tag{4}$$

$$G_V = G_K - G_{K'} \tag{5}$$
$$G_S = G_{\uparrow\uparrow} - G_{\uparrow\downarrow} \tag{6}$$

Using the function, Lm(μ), electronic thermal conductance,

K_e, and Seebeck coefficient, S, are calculated [51], [52]:

$$L_m = \frac{2}{h}\int_{E_F}^{E_F+\hbar\omega}\int_{-\pi/2}^{\pi/2} \Gamma_{withphoton}(E).(E-\mu)^m.\left(-\frac{\partial f_{FD}(E)}{\partial E}\right) .\cos\theta d\theta dE \tag{7}$$

$$K_e = \frac{1}{T}\left(L_2 - \frac{L_1^2}{L_0}\right) \tag{8}$$

$$S = \frac{1}{eT}.\frac{L_1}{L_0} \tag{9}$$

where (m = 0, 1, 2), $\hbar$, μ, T, and e are reduced Planck's constant, electrochemical potential, absolute temperature and electronic charge [8], [10], [51], [52] and $\left(-\frac{\partial f_{FD}}{\partial E}\right)$ represents first derivative of Fermi-Dirac distribution function.

The thermoelectric figure of merit, ZT, of present nanodevice will be given as [8], [10], [51], [52]:

$$ZT = \frac{S^2 G T}{K_e + K_L} \tag{10}$$

where K_L is the lattice (phonon) thermal conductance.

Of single-layer silicene, the intrinsic lattice thermal conductivity is 9.4W/mK much smaller than that of bulk silicon or graphene at room temperature [53]–[55]. It is well known that interfaces impact on thermal conductivity in superlattices can have different sources, including specular scattering because of acoustic mismatch [56], phonon localization and bandgap formation [57]. This is supposed to lead to a greater decrease in thermal conductivity than that in electrical conductivity because of lower mobility. For the optimization of electronic transport, superlattices can be engineered by controlling quantum confinements, band offsets and tunneling processes among different material layers [58], [59]. Therefore, it is of present and imminent interest to design suitable superlattices with the purpose of optimizing thermoelectric performance. Hence the calculations will be performed at low temperatures as will be shown in the results below. Then thermoelectric figure of merit, ZT, of this device will be calculated as [27], [45]:

$$ZT = \frac{S^2 G T}{K_e} \tag{11}$$

In silicene the Seebeck coefficient, S, classified into two cases:

Valley resolved Seebeck coefficient, $S_{K(K')}$, is:

$$S_{K(K')} = S_{K(K')\uparrow\uparrow} + S_{K(K')\uparrow\downarrow} \tag{12}$$

Spin resolved Seebeck coefficient, $S_{\uparrow\uparrow(\uparrow\downarrow)}$, is:

$$S_{\uparrow\uparrow(\uparrow\downarrow)} = S_{K\uparrow\uparrow(\uparrow\downarrow)} + S_{K'\uparrow\uparrow(\uparrow\downarrow)} \tag{13}$$

The charge Seebeck coefficient is computed as [60]:

$$S_c = \frac{1}{2}(S_{\uparrow\uparrow} + S_{\uparrow\downarrow}) \tag{14}$$

The spin Seebeck coefficient is computed as [60]:

$$S_S = (S_{\uparrow\uparrow} - S_{\uparrow\downarrow}) \tag{15}$$

Also, the valley Seebeck coefficient, SV, in analogy with SS can be defined as:

$$S_V = S_K - S_{K'} \tag{16}$$

The charge electronic thermal conductance also, is computed as [60]:

$$K_{ec} = \frac{1}{2}\left(K_{e\uparrow\uparrow} + K_{e\uparrow\downarrow}\right) \tag{17}$$

The valley and spin electronic thermal conductance are computed as [60]:

$$K_{eV} = K_{eK} - K_{eK'} \tag{18}$$
$$K_{eS} = = (K_{e\uparrow\uparrow} - K_{e\uparrow\downarrow}) \tag{19}$$

For electricity generation, the thermoelectric device ideal efficiency, η, is [8]–[11]:

$$\eta = \eta_c \frac{\sqrt{1+ZT}-1}{\sqrt{1+ZT}-(\frac{T_c}{T_h})} \tag{20}$$

where T_h and T_c are the temperatures of hot side (heat source) and cold side (heat sink), respectively, of the proposed device and η_c represents Carnot efficiency and η_c = 1- T_c/T_h. The figure of merit relates the efficiency of device through Eq.(20) which is a materials property, so a lot of thermoelectric field's work is provided to materials development for enhancement of thermal electrical conversion efficiency. The charge, spin, valley efficiency, η_c, η_s, *and* η_V will be computed as shown below.

The Nernst coefficient, N_T, is expressed as [10], [51], [61]:

$$N_T = \frac{1}{8\pi k_B T^2}\int_{E_F}^{E_F+\hbar\omega}\int_{-\pi/2}^{\pi/2} \Gamma_{withphoton}(E).(E-\mu) .\left(-\frac{\partial f_{FD}(E)}{\partial E}\right).\left(1+\frac{\partial f_{FD}(E)}{\partial E}\right).\cos\theta d\theta dE \tag{21}$$

$$\left(-\frac{\partial f_{FD}}{\partial E}\right) = (4k_BT)^{-1}\cosh^{-2}\left(\frac{E-E'_F+n\hbar\omega}{2k_BT}\right) \tag{22}$$

where k_B is Boltzmann constant and $\left(-\frac{\partial f_{FD}}{\partial E}\right)$ represents first derivative of Fermi-Dirac distribution function. The charge, spin, valley Nernst coefficients will be given as respectively:

$$N_{cT} = \frac{1}{2}\left(N_{T\uparrow\uparrow} + N_{T\uparrow\downarrow}\right) \tag{23}$$
$$N_{ST} = \left(N_{T\uparrow\uparrow} - N_{T\uparrow\downarrow}\right) \tag{24}$$
$$N_{VT} = (N_{KT} - N_{K'T}) \tag{25}$$

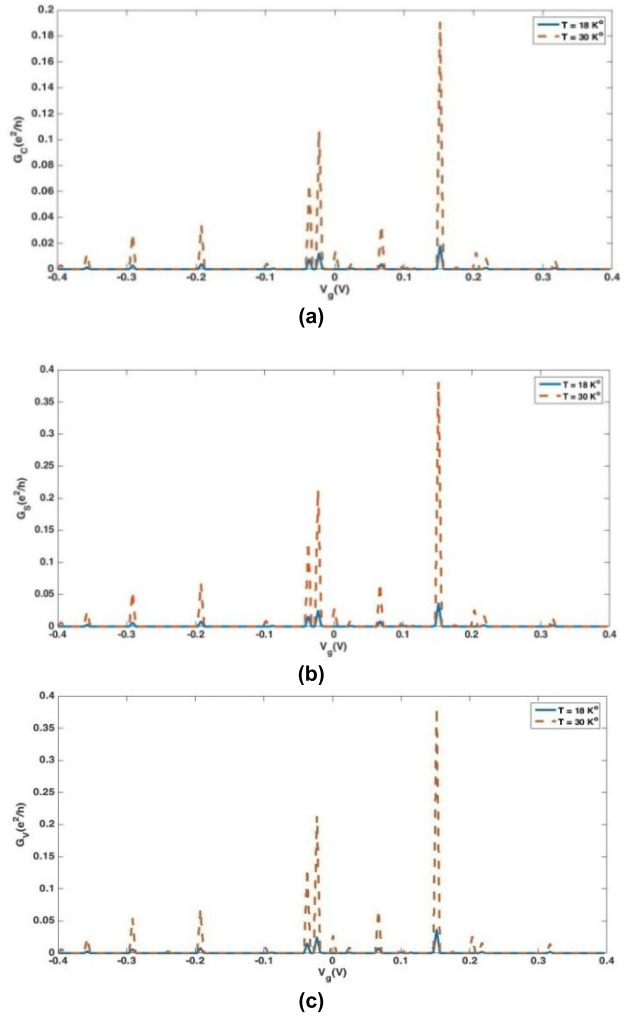

FIGURE 2. The variation of electric resolved conductance versus, V_g, at both temperatures for (a) charge, (b) spin, and (c) valley.

III. RESULTS AND DISCUSSIONS

Thermal power parameters of the explored silicene-based nanostructure model are computed numerically by taking N = 1 which means that the nanostructure is a lead of normal silicene before a (ferromagnetic /normal / ferromagnetic strips of silicene) then a lead of normal silicene. The parameters' values are as follow [35], [36], [39], [45], [50]:

ac-field peak	$V_{ac} = 0.25$ V
Fermi velocity	$v_F \approx 5.5 \times 10^5$ m/s
Lande g-factor	$g = 2$
intrinsic spin-orbit coupling	$\lambda_{SO} = 3.9\,meV$
on-site potential difference between A and B sublattices	$\Delta_z = 2$ meV
y-directionjunction	d = 30nm
width	W = 20nm
barrier height	$V_b = 50$ meV

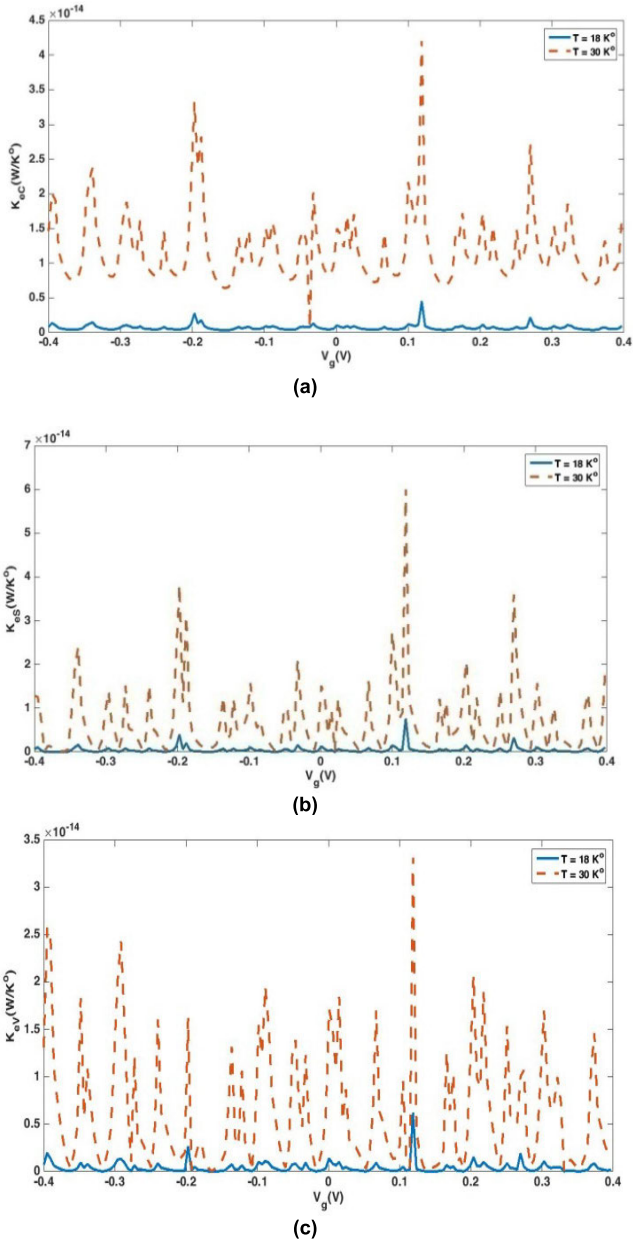

FIGURE 3. The electronic thermal conductance variation versus, V_g, at both temperatures for (a) charge, (b) spin, and (c) valley.

The external applied magnetic field of 0.1T is taken as an optimum value in the tested model [46], [51]. The quasiparticle Dirac fermions carrier density, n', is used by (Eq.26) to compute the modulated Fermi energy, E'_F [45], [54], [60].

$$E'_F = \sqrt{\pi}\,\hbar\, v_F \sqrt{n'} \tag{26}$$

Since the parameter n′ is tuned by proximity effect of single layer ferromagnetic silicene [45], [54], [61] then, the parameter, n′, is determined by the theory of density function to get the optimum magnitude of E'_F. The usual electric field resulted from gate voltage, V_g, could modulate the previously mentioned parameters which generates possibilities for tunable energy gap applications.

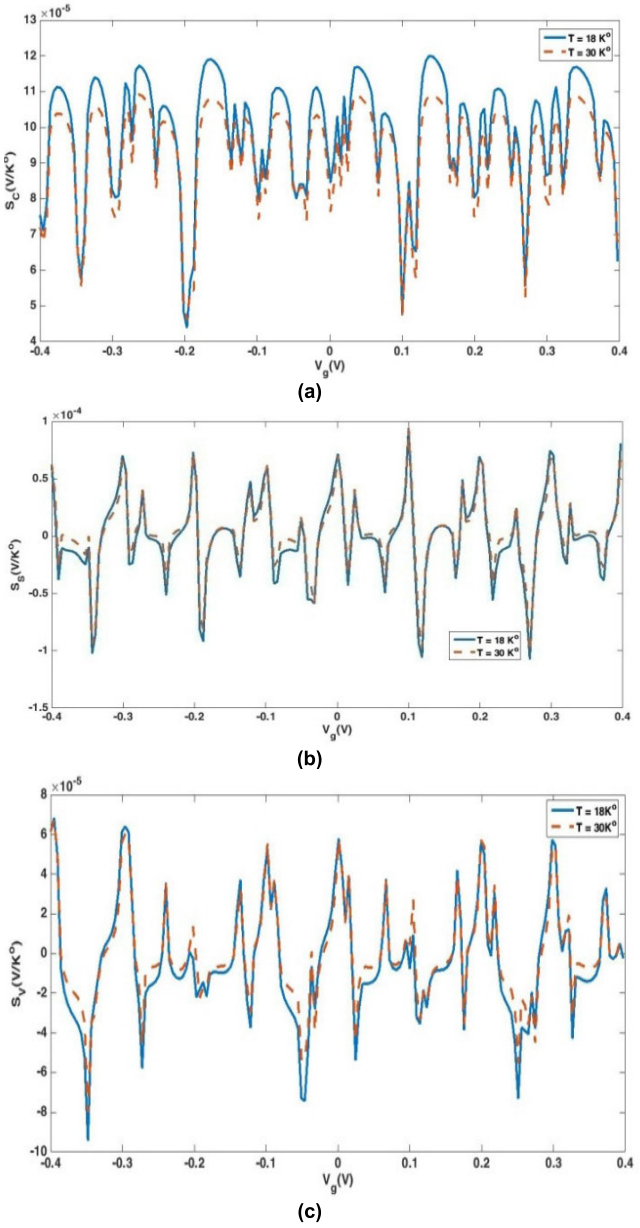

FIGURE 4. The Seebeck coefficient variation versus, V_g, at both temperatures for (a) charge, (b) spin, and (c) valley.

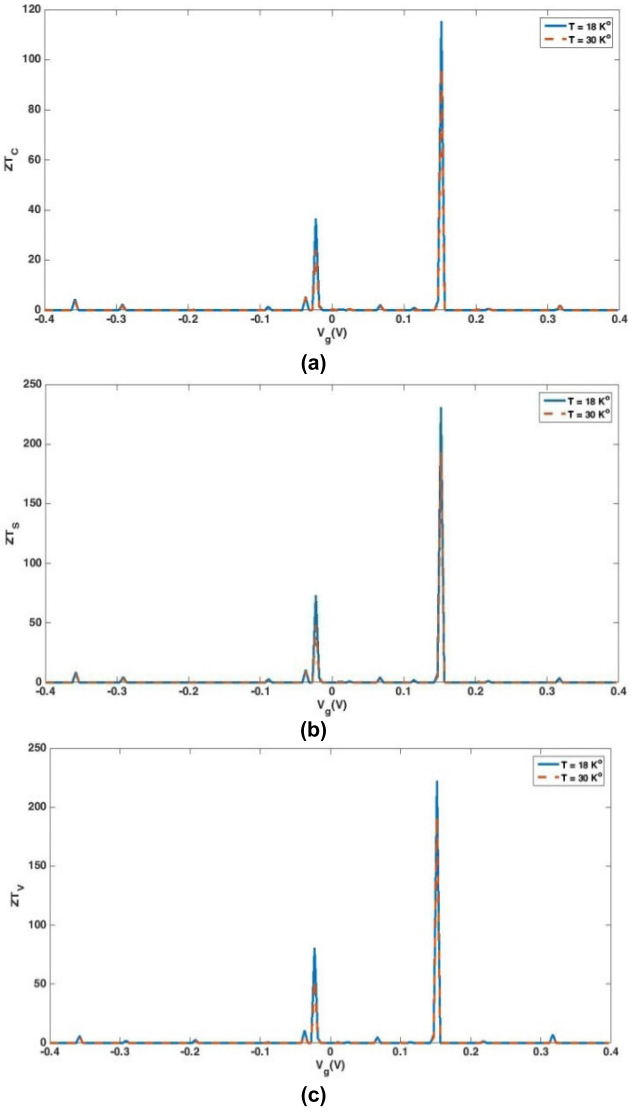

FIGURE 5. The figure of merit variation versus, V_g, at both temperatures for (a) charge, (b) spin, and (c) valley.

The IR range is supposed to be the best range to enrich the thermoelectric parameters of explored nanostructure, so the induced ac-field frequency choose to be 1.25THz [27], [45]. All figures plotted against gate voltage at different two temperatures, $T_c = 18K$ and $T_h = 30K$.

Fig.2 declares the electric conductance in terms of (e^2/h) for case of charge (a), spin (b) and valley (c) versus, Vg, at the both temperatures. It exhibits a selective behavior at specific values of, V_g, with maxima at 0.1519V and equals $0.01854(e^2/h)$ at 18K and equals $0.1907(e^2/h)$ at 30K for charge electric conductance, while for spin electric conductance and valley electric conductance they show the same behavior with maxima at 0.1519V and equals $0.03708(e^2/h)$ at 18K and equals $0.3813(e^2/h)$ at 30K. Also, the widths of such oscillations and its peak height might be controlled by magnetic proximity effect and electric field of EuO ferromagnetic insulator [22], [23], [42], [45], [62].

Fig.3 declares the variation of electronic thermal conductance in terms of (W/K) for case of charge (a), spin (b) and valley (c) versus, Vg, at both temperatures. It is obvious that as the temperature rises, electronic thermal conductance increases. and shows multi peaks with maxima $4.204*10^{-14}$ W/K at 30K and $4.512*10^{-15}$ W/K at 18K for charge electronic thermal conductance, $6.007*10^{-14}$ W/K at 30K and $7.674*10^{-15}$ W/K at 18K for spin electronic thermal conductance and $3.312*10^{-14}$ W/K at 30K and $6.235*10^{-15}$ W/K at 18K for valley electronic thermal conductance. All maxima take place at 0.1189 V.

Fig.4 declares the variation of Seebeck coefficient in terms of (V/K) for case of charge (a), spin (b) and valley

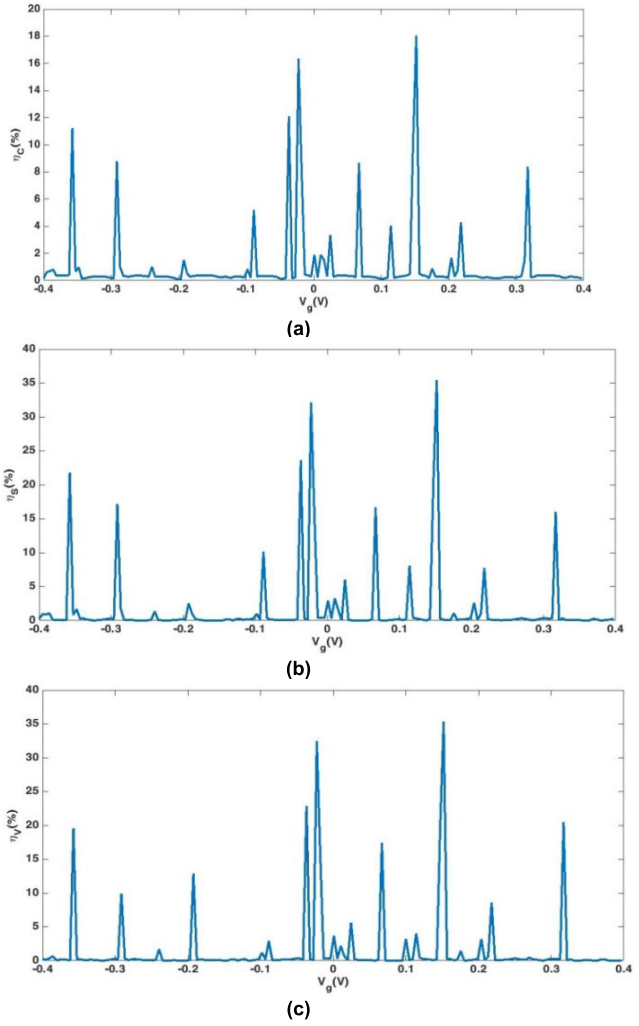

FIGURE 6. The conversion efficiency variation versus, V_g, at both temperatures for (a) charge, (b) spin, and (c) valley.

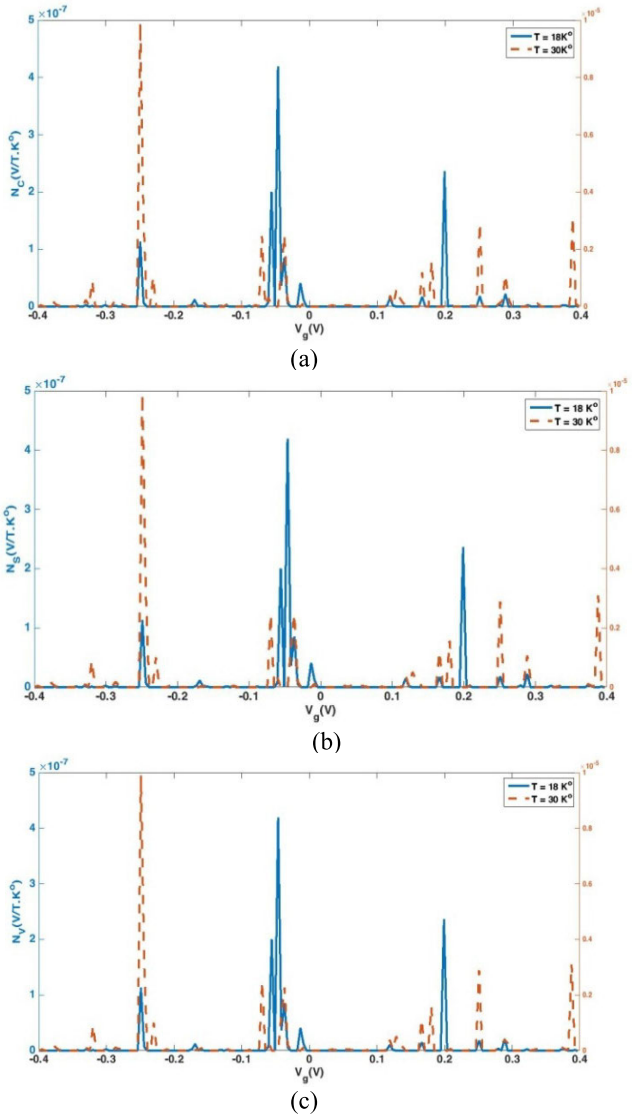

FIGURE 7. Nernst coefficient variation versus, V_g, at both temperatures for (a) charge, (b) spin, and (c) valley.

(c) versus, Vg, at the both temperatures. It demonstrates a periodic like manner and temperature insensitive in this range. The charge Seebeck coefficient varies from $4.384*10^{-5}$ to $1.19*10^{-4}$V/K, the spin Seebeck coefficient varies from $-1.074*10^{-4}$ to $9.403*10^{-5}$V/K and the valley Seebeck coefficient varies from $-9.437*10^{-5}$ to $6.744*10^{-5}$V/K. Also, it is shown from this figure that Seebeck coefficient magnitudes (charge, spin, valley) are quite high. This is because of quantum confinement effects of this nanostructure [26], [42], [45], [58], [59], [63]–[65].

Fig.5 declares the variation of figure of merit for case of charge (a), spin (b) and valley (c) versus, Vg, at the both temperatures. It demonstrates a sharp selective behavior at specific gate voltage magnitudes with two noticeable maxima at 0.1519V with $ZT_C = 115.4$ at 18K, $ZT_C = 96.56$ at 30K and at -0.0226V with $ZT_C = 36.75$ at 18K, $ZT_C = 24.15$ at 30K for charge figure of merit, while for spin figure of merit and valley figure of merit they show the same behavior with maxima at 0.1519V with $ZT_S = ZT_V = 230.8$ at 18K, $ZT_S = ZT_V = 193$ at 30K and at -0.0226V with $ZT_S = ZT_V = 73.46$ at 18K, $ZT_S = ZT_V = 48.3$ at 30K.

Fig.6 declares the conversion efficiency for case of charge (a), spin (b) and valley (c) versus, Vg. It shows a selective behavior with periodic like nature and has maximum at 0.1519V equals 18.07% for charge case. While for spin and valley cases they show the same behavior with maximum at 0.1519V and equals 35.44%. Also, Figs. (5,6) demonstrate that figure of merits magnitudes (charge, spin, valley) are larger than one at some values of gate voltage. This figure of merits improvement is because of enhancement of corresponding Seebeck coefficients (Fig.4) [50], [66]. So in the present results show that ferromagnetic silicene superlattice whose minibands are formed with specific bandwidth segregated by forbidden bands [45], [59] because of which an optimal density of states pattern to provide thermoelectric

figure of merit enrichment results and the corresponding quite high values for thermoelectric efficiencies (Fig.6).

-Fig.7 declares the Nernst coefficient in terms of (V/T.K) for case of charge (a), spin (b) and valley (c) versus, Vg, at the both temperatures. It demonstrates a selective behavior at specific magnitudes of gate voltage with maxima at -0.04623V and equals $2.098*10^{-7}$V/T.K at 18K and at -0.2491V equals $4.949*10^{-6}$V/T.K at 30K for charge Nernst coefficient, while for spin Nernst coefficient and valley Nernst coefficient they show the same behavior with maximum at -0.04623V and equals $4.196*10^{-7}$V/T.K at 18K and at -0.2491V equals $9.898*10^{-6}$V/T.K at 30K. It is shown from Fig.(7) that Nernst coefficients magnitude (charge, spin, valley) are quite high at certain values of the gate voltage. This enhancement of present Nernst coefficients might be due the effects of the applied electric current and ferromagnetic exchange magnetic field of the ferromagnetic silicene [67], [68]. Also, the modulation of Fermi energy and strong spin orbit coupling of silicene might play an important role for enhancement of Nernst coefficients (charge, spin, and valley).

IV. CONCLUSION

The ferromagnetic silicene superlattice valley-spin thermoelectric transport properties are investigated at different temperatures. Since Nernst coefficient represents the natural manifestation of electric current normal to temperature gradient and magnetic field, then spin-valley Nernst coefficients of the present nanodevice are also investigated. Results demonstrate that the computed thermoelectric parameters and Nernst coefficient are enriched to very acceptable values with high thermoelectric efficiency. According to this work, for high-efficiency energy harvesting nanodevices and flexible thermoelectric power generation, ferromagnetic silicene superlattice is very promising.

REFERENCES

[1] A. M. Shaheen, R. A. El-Sehiemy, E. E. Elattar, and A. S. Abd-Elrazek, "A modified crow search optimizer for solving non-linear OPF problem with emissions," *IEEE Access*, vol. 9, pp. 43107–43120, 2021, doi: 10.1109/ACCESS.2021.3060710.

[2] A. S. Bayoumi, R. A. El-Sehiemy, K. Mahmoud, M. Lehtonen, and M. M. F. Darwish, "Assessment of an improved three-diode against modified two-diode patterns of MCS solar cells associated with soft parameter estimation paradigms," *Appl. Sci.*, vol. 11, no. 3, p. 1055, Jan. 2021, doi: 10.3390/app11031055.

[3] A. M. Shaheen, E. E. Elattar, R. A. El-Sehiemy, and A. M. Elsayed, "An improved sunflower optimization algorithm-based Monte Carlo simulation for efficiency improvement of radial distribution systems considering wind power uncertainty," *IEEE Access*, vol. 9, pp. 2332–2344, 2021, doi: 10.1109/ACCESS.2020.3047671.

[4] A. M. Shaheen, A. R. Ginidi, R. A. El-Sehiemy, and E. E. Elattar, "Optimal economic power and heat dispatch in cogeneration systems including wind power," *Energy*, vol. 225, Jun. 2021, Art. no. 120263, doi: 10.1016/j.energy.2021.120263.

[5] A. A. Abou El Ela, R. A. El-Sehiemy, A. M. Shaheen, and A. S. Shalaby, "Application of the crow search algorithm for economic environmental dispatch," in *Proc. 19th Int. Middle East Power Syst. Conf. (MEPCON)*, Dec. 2017, pp. 78–83, doi: 10.1109/MEPCON.2017.8301166.

[6] A. A. Abou El-Ela, M. A. Bishr, S. M. Allam, and R. A. El-Sehiemy, "An emergency power system control based on the multi-stage fuzzy based procedure," *Electr. Power Syst. Res.*, vol. 77, nos. 5–6, pp. 421–429, Apr. 2007, doi: 10.1016/j.epsr.2006.04.004.

[7] A. Abaza, A. Fawzy, R. A. El-Sehiemy, A. S. Alghamdi, and S. Kamel, "Sensitive reactive power dispatch solution accomplished with renewable energy allocation using an enhanced coyote optimization algorithm," *Ain Shams Eng. J.*, vol. 12, no. 2, pp. 1723–1739, Jun. 2021, doi: 10.1016/j.asej.2020.08.021.

[8] Z.-G. Chen, G. Han, L. Yang, L. Cheng, and J. Zou, "Nanostructured thermoelectric materials: Current research and future challenge," *Prog. Natural Sci., Mater. Int.*, vol. 22, no. 6, pp. 535–549, Dec. 2012, doi: 10.1016/j.pnsc.2012.11.011.

[9] T. Zhu, Y. Liu, C. Fu, J. P. Heremans, J. G. Snyder, and X. Zhao, "Compromise and synergy in high-efficiency thermoelectric materials," *Adv. Mater.*, vol. 29, no. 30, Aug. 2017, Art. no. 1605884.

[10] H. J. Goldsmid, *Introduction to Thermoelectricity*, 2nd ed. Berlin, Germany: Springer-Verlag, 2016.

[11] H. E. Katz and T. O. Poehler, *Innovative Thermoelectric Materials*. London, U.K.: Imperial College Press, 2016.

[12] H. A. El-Demsisy, M. D. Asham, D. S. Louis, and A. H. Phillips, "Thermoelectric seebeck and peltier effects of single walled carbon nanotube quantum dot nanodevice," *Carbon Lett.*, vol. 21, pp. 8–15, Jan. 2017, doi: 10.5714/CL.2017.21.008.

[13] C. J. Vineis, A. Shakouri, A. Majumdar, and M. G. Kanatzidis, "Nanostructured thermoelectrics: Big efficiency gains from small features," *Adv. Mater.*, vol. 22, no. 36, pp. 3970–3980, Sep. 2010, doi: 10.1002/adma.201000839.

[14] G. Zhang, Q. Yu, W. Wang, and X. Li, "Nanostructures for thermoelectric applications: Synthesis, growth mechanism, and property studies," *Adv. Mater.*, vol. 22, no. 17, pp. 1959–1962, May 2010, doi: 10.1002/adma.200903812.

[15] S. Twaha, J. Zhu, Y. Yan, and B. Li, "A comprehensive review of thermoelectric technology: Materials, applications, modelling and performance improvement," *Renew. Sustain. Energy Rev.*, vol. 65, pp. 698–726, Nov. 2016, doi: 10.1016/j.rser.2016.07.034.

[16] Y. Ouyang, Z. Zhang, D. Li, J. Chen, and G. Zhang, "Emerging theory, materials, and screening methods: New opportunities for promoting thermoelectric performance," *Ann. Phys.*, vol. 531, no. 4, Apr. 2019, Art. no. 1800437, doi: 10.1002/andp.201800437.

[17] I. Žutić, J. Fabian, and S. Das Sarma, "Spintronics: Fundamentals and applications," *Rev. Mod. Phys.*, vol. 76, no. 2, pp. 323–410, Apr. 2004, doi: 10.1103/RevModPhys.76.323.

[18] Y. Xu, D. D. Awschalom, and J. Nitta, *Handbook of Spintronics*. Berlin, Germany: Springer-Verlag, 2015.

[19] A. S. Abdelrazek, W. A. Zein, and A. H. Phillips, "Spin-dependent goos–hanchen effect in semiconducting quantum dots," *SPIN*, vol. 3, no. 2, Jun. 2013, Art. no. 1350007, doi: 10.1142/S2010324713500070.

[20] Z. Yu, H. Pan, and Y. Yao, "Electric field controlled spin-and valley-polarized edge states in silicene with extrinsic Rashba effect," *Phys. Rev. B, Condens. Matter*, vol. 92, no. 15, Oct. 2015, Art. no. 155419, doi: 10.1103/PhysRevB.92.155419.

[21] V. Vargiamidis and P. Vasilopoulos, "Polarized spin and valley transport across ferromagnetic silicene junctions," *J. Appl. Phys.*, vol. 117, no. 9, Mar. 2015, Art. no. 094305, doi: 10.1063/1.4913934.

[22] I. S. Ahmed, M. D. Asham, and A. H. Phillips, "Coherent Spin-valley polarization characteristics of silicene field effect transistor," *J. Multidiscip. Eng. Sci. Technol.*, vol. 4, no. 2, pp. 6701–6708, 2017.

[23] I. S. Ahmed, M. D. Asham, and A. H. Phillips, "Spin-valleytronics of silicene based nanodevices (SBNs)," *J. Magn. Magn. Mater.*, vol. 456, pp. 199–203, Jun. 2018, doi: 10.1016/j.jmmm.2018.02.028.

[24] M. D. Asham and A. H. Phillips, "Coherent spin transport properties of ferromagnetic graphene superlattice unit cell," *Phys. E, Low-dimensional Syst. Nanostruct.*, vol. 113, pp. 97–102, Sep. 2019, doi: 10.1016/j.physe.2019.05.003.

[25] A. S. Abdelrazek and A. H. Phillips, "Spin coherent transport in graphene superlattice based nanostructure," *Spin*, vol. 6, no. 6, pp. 10190–10196, 2019.

[26] N. Missault, P. Vasilopoulos, F. M. Peeters, and B. Van Duppen, "Spin- and valley-dependent miniband structure and transport in silicene superlattices," *Phys. Rev. B, Condens. Matter*, vol. 93, no. 12, Mar. 2016, Art. no. 125425, doi: 10.1103/PhysRevB.93.125425.

[27] M. M. El-Banna, A. H. Phillips, and A. S. A. Bayoumi, "Spin-valley thermoelectric characteristics of ferromagnetic silicene superlattice," *Ain Shams Eng. J.*, vol. 12, no. 2, pp. 2193–2203, Jun. 2021, doi: 10.1016/j.asej.2021.01.002.

[28] J.-F. Liu, W.-J. Deng, K. Xia, C. Zhang, and Z. Ma, "Transport of spin-polarized electrons in a magnetic superlattice," *Phys. Rev. B, Condens. Matter*, vol. 73, no. 15, Apr. 2006, Art. no. 155309, doi: 10.1103/PhysRevB.73.155309.

[29] P.-F. Yang and Y. Guo, "Spin-dependent tunneling time in periodic diluted-magnetic-semiconductor/nonmagnetic-barrier superlattices," *Appl. Phys. Lett.*, vol. 108, no. 5, Feb. 2016, Art. no. 052402, doi: 10.1063/1.4941302.

[30] J.-C. Le Breton, S. Sharma, H. Saito, S. Yuasa, and R. Jansen, "Thermal spin current from a ferromagnet to silicon by seebeck spin tunnelling," *Nature*, vol. 475, no. 7354, pp. 82–85, Jul. 2011, doi: 10.1038/nature10224.

[31] Y. Pu, E. Johnston-Halperin, D. D. Awschalom, and J. Shi, "Anisotropic thermopower and planar nernst effect in $Ga_{1-x}Mn_xAs$ ferromagnetic semiconductors," *Phys. Rev. Lett.*, vol. 97, no. 3, Jul. 2006, Art. no. 036601, doi: 10.1103/PhysRevLett.97.036601.

[32] S. Y. Huang, W. G. Wang, S. F. Lee, J. Kwo, and C. L. Chien, "Intrinsic spin-dependent thermal transport," *Phys. Rev. Lett.*, vol. 107, no. 21, Nov. 2011, Art. no. 216604, doi: 10.1103/PhysRevLett.107.216604.

[33] M. Hatami, G. E. W. Bauer, Q. Zhang, and P. J. Kelly, "Thermal spin-transfer torque in magnetoelectronic devices," *Phys. Rev. Lett.*, vol. 99, no. 6, Aug. 2007, Art. no. 066603, doi: 10.1103/PhysRevLett.99.066603.

[34] A. Slachter, F. L. Bakker, J.-P. Adam, and B. J. van Wees, "Thermally driven spin injection from a ferromagnet into a non-magnetic metal," *Nature Phys.*, vol. 6, no. 11, pp. 879–882, Nov. 2010, doi: 10.1038/nphys1767.

[35] X.-Q. Yu, Z.-G. Zhu, G. Su, and A.-P. Jauho, "Thermally driven pure spin and valley currents via the anomalous nernst effect in monolayer group-VI dichalcogenides," *Phys. Rev. Lett.*, vol. 115, no. 24, Dec. 2015, Art. no. 246601, doi: 10.1103/PhysRevLett.115.246601.

[36] G. Sharma, "Tunable topological nernst effect in two-dimensional transition-metal dichalcogenides," *Phys. Rev. B, Condens. Matter*, vol. 98, no. 7, Aug. 2018, Art. no. 075416, doi: 10.1103/PhysRevB.98.075416.

[37] M. T. Dau, C. Vergnaud, A. Marty, C. Beigné, S. Gambarelli, V. Maurel, T. Journot, B. Hyot, T. Guillet, B. Grévin, H. Okuno, and M. Jamet, "The valley nernst effect in WSe_2," *Nature Commun.*, vol. 10, no. 1, Dec. 2019, Art. no. 5796, doi: 10.1038/s41467-019-13590-8.

[38] S. Meyer, Y.-T. Chen, S. Wimmer, M. Althammer, T. Wimmer, R. Schlitz, S. Geprägs, H. Huebl, D. Ködderitzsch, H. Ebert, G. E. W. Bauer, R. Gross, and S. T. B. Goennenwein, "Observation of the spin nernst effect," *Nature Mater.*, vol. 16, no. 10, pp. 977–981, Oct. 2017, doi: 10.1038/NMAT4964.

[39] P. Sheng, Y. Sakuraba, Y.-C. Lau, S. Takahashi, S. Mitani, and M. Hayashi, "The spin nernst effect in tungsten," *Sci. Adv.*, vol. 3, no. 11, Nov. 2017, Art. no. e1701503, doi: 10.1126/sciadv.1701503.

[40] E. Cinquanta, E. Scalise, D. Chiappe, C. Grazianetti, B. van den Broek, M. Houssa, M. Fanciulli, and A. Molle, "Getting through the nature of silicene: An sp^2–sp^3 two-dimensional silicon nanosheet," *J. Phys. Chem. C*, vol. 117, no. 32, pp. 16719–16724, Aug. 2013, doi: 10.1021/jp405642g.

[41] D. Zha, C. Chen, and J. Wu, "Electronic transport through a silicene-based zigzag and armchair junction," *Solid State Commun.*, vol. 219, pp. 21–24, Oct. 2015, doi: 10.1016/j.ssc.2015.06.018.

[42] J. Zhao, H. Liu, Z. Yu, R. Quhe, S. Zhou, Y. Wang, C. C. Liu, H. Zhong, N. Han, J. Lu, Y. Yao, and K. Wu, "Rise of silicene: A competitive 2D material," *Prog. Mater. Sci.*, vol. 83, pp. 124–151, Oct. 2016, doi: 10.1016/j.pmatsci.2016.04.001.

[43] Y. Liu, C. Zeng, J. Zhong, J. Ding, Z. M. Wang, and Z. Liu, "Spintronics in two-dimensional materials," *Nano-Micro Lett.*, vol. 12, no. 1, Dec. 2020, Art. no. 93, doi: 10.1007/s40820-020-00424-2.

[44] L. Tao, E. Cinquanta, D. Chiappe, C. Grazianetti, M. Fanciulli, M. Dubey, A. Molle, and D. Akinwande, "Silicene field-effect transistors operating at room temperature," *Nature Nanotechnol.*, vol. 10, no. 3, pp. 227–231, Mar. 2015, doi: 10.1038/nnano.2014.325.

[45] A. S. A. Bayoumi and A. H. Phillips, "Transport properties of ferromagnetic silicene superlattice based nanostructure," in *Recent Advances in Engineering Mathematics and Physics*. Springer, 2020, pp. 101–115, doi: 10.1007/978-3-030-39847-7_8.

[46] M. D. Asham, W. A. Zein, and A. H. Phillips, "Photo-induced spin dynamics in nanoelectronic devices," *Chin. Phys. Lett.*, vol. 29, no. 10, Oct. 2012, Art. no. 108502, doi: 10.1088/0256-307X/29/10/108502.

[47] A. S. Abdelrazek, M. M. El-Banna, and A. H. Phillips, "Photon-spin coherent manipulation of piezotronic nanodevice," *Micro Nano Lett.*, vol. 11, no. 12, pp. 876–880, Dec. 2016, doi: 10.1049/mnl.2016.0264.

[48] H. J. Goldsmid, *The Physics of Thermoelectric Energy Conversion*. San Rafael, CA, USA: Morgan & Claypool, 2017.

[49] M. Dragoman and D. Dragoman, *2D Nanoelectronics, Physics and Devices of Atomically Thin Materials*. Springer, 2017.

[50] D. Li, Y. Gong, Y. Chen, J. Lin, Q. Khan, Y. Zhang, Y. Li, H. Zhang, and H. Xie, "Recent progress of two-dimensional thermoelectric materials," *Nano-Micro Lett.*, vol. 12, no. 1, Dec. 2020, Art. no. 36, doi: 10.1007/s40820-020-0374-x.

[51] J.-S. Wang, J. Wang, and J. T. Lü, "Quantum thermal transport in nanostructures," *Eur. Phys. J. B*, vol. 62, no. 4, pp. 381–404, Apr. 2008, doi: 10.1140/epjb/e2008-00195-8.

[52] I. S. Ahmed, M. D. Asham, and A. H. Phillips, "Spin thermoelectric effect of diluted magnetic semiconductor nanodevice," *Spin*, vol. 3, no. 4, pp. 1–6, 2016.

[53] B. Liu, C. D. Reddy, J. Jiang, H. Zhu, J. A. Baimova, S. V. Dmitriev, and K. Zhou, "Thermal conductivity of silicene nanosheets and the effect of isotopic doping," *J. Phys. D, Appl. Phys.*, vol. 47, no. 16, Apr. 2014, Art. no. 165301, doi: 10.1088/0022-3727/47/16/165301.

[54] Z. Wang, T. Feng, and X. Ruan, "Thermal conductivity and spectral phonon properties of freestanding and supported silicene," *J. Appl. Phys.*, vol. 117, no. 8, Feb. 2015, Art. no. 084317, doi: 10.1063/1.4913600.

[55] H. Xie, M. Hu, and H. Bao, "Thermal conductivity of silicene from first-principles," *Appl. Phys. Lett.*, vol. 104, no. 13, Mar. 2014, Art. no. 131906.

[56] G. Chen, "Thermal conductivity and ballistic-phonon transport in the cross-plane direction of superlattices," *Phys. Rev. B, Condens. Matter*, vol. 57, no. 23, pp. 14958–14973, Jun. 1998, doi: 10.1103/PhysRevB.57.14958.

[57] R. Venkatasubramanian, "Lattice thermal conductivity reduction and phonon localizationlike behavior in superlattice structures," *Phys. Rev. B, Condens. Matter*, vol. 61, no. 4, pp. 3091–3097, Jan. 2000, doi: 10.1103/PhysRevB.61.3091.

[58] X. Wang, Y. Hong, P. K. L. Chan, and J. Zhang, "Phonon thermal transport in silicene-germanene superlattice: A molecular dynamics study," *Nanotechnology*, vol. 28, no. 25, Jun. 2017, Art. no. 255403, doi: 10.1088/1361-6528/aa71fa.

[59] P. Priyadarshi, A. Sharma, S. Mukherjee, and B. Muralidharan, "Superlattice design for optimal thermoelectric generator performance," *J. Phys. D, Appl. Phys.*, vol. 51, no. 18, May 2018, Art. no. 185301, doi: 10.1088/1361-6463/aab8d5.

[60] R. Świrkowicz, M. Wierzbicki, and J. Barnaś, "Thermoelectric effects in transport through quantum dots attached to ferromagnetic leads with noncollinear magnetic moments," *Phys. Rev. B, Condens. Matter*, vol. 80, no. 19, Nov. 2009, Art. no. 195409, doi: 10.1103/PhysRevB.80.195409.

[61] W. S. Mohamed, M. D. Asham, and A. H. Phillips, "Photo-thermoelectric effect of graphene nanoribbon nanodevice," *J. Multidisciplinary Eng. Sci. Technol.*, vol. 4, no. 2, pp. 6720–6725, 2017.

[62] T. Yokoyama, "Controllable valley and spin transport in ferromagnetic silicene junctions," *Phys. Rev. B, Condens. Matter*, vol. 87, no. 24, Jun. 2013, Art. no. 241409, doi: 10.1103/PhysRevB.87.241409.

[63] A. M. Elseddawy, A. H. Phillips, and A. S. Bayoumi, "Carbon nanotube-based nanoelectromechanical resonator as mass biosensor," *Chin. Phys. B*, vol. 29, no. 7, Jul. 2020, Art. no. 078501, doi: 10.1088/1674-1056/ab888f.

[64] M. Hu and D. Poulikakos, "Si/Ge superlattice nanowires with ultralow thermal conductivity," *Nano Lett.*, vol. 12, no. 11, pp. 5487–5494, Nov. 2012, doi: 10.1021/nl301971k.

[65] L. Shi, J. Jiang, G. Zhang, and B. Li, "High thermoelectric figure of merit in silicon-germanium superlattice structured nanowires," *Appl. Phys. Lett.*, vol. 101, no. 23, Dec. 2012, Art. no. 233114.

[66] O. Oubram, O. Navarro, E. J. Guzmán, and I. Rodríguez-Vargas, "Effects of disorder on the transport and thermoelectric properties of silicene superlattices," *Phys. E, Low-Dimensional Syst. Nanostruct.*, vol. 120, Jun. 2020, Art. no. 114100, doi: 10.1016/j.physe.2020.114100.

[67] J. Zheng, J.-J. Jin, X. Zhao, C.-L. Li, and Y. Guo, "Spin and charge nernst effects in four-terminal ferromagnetic graphene," *Spin*, vol. 8, no. 1, Mar. 2018, Art. no. 1840001, doi: 10.1142/S2010324718400015.

[68] A. Das, H. Mishra, and R. K. Mohapatra, "Magneto-seebeck coefficient and nernst coefficient of a hot and dense hadron gas," *Phys. Rev. D, Fields*, vol. 102, no. 1, Jul. 2020, Art. no. 014030, doi: 10.1103/PhysRevD.102.014030.

MOHAMMED M. EL-BANNA received the B.Sc. degree in electronics and communication engineering from Ain Shams University (ASU), Cairo, Egypt, and the M.Sc. and Ph.D. degrees from the Engineering Physics Department, Faculty of Engineering (FE), ASU, in 2006 and 2011, respectively. He is currently an Associate Professor with the Engineering Physics and Mathematics Department, FE, ASU. His research interests include semiconductor physics, characterization, simulation and modeling of nanoscale devices, semiconductor power devices, solar cells, 3-D detectors, spin dependence transport in semiconducting nanowires, and two dimensional materials (graphene, silicene).

ADEL HELMY PHILLIPS is currently a Professor of theoretical physics with the Faculty of Engineering, Ain Shams University. He has published 111 articles in many international journals. He is the author of the following book chapter ''Nanotechnology and Semiconductor Nanodevices'' in a book *Hadron Models and Related New Energy Issues* edited by F. Smarandache and V. Christiano (USA: InfoLearn Quest, November 2007). Many research students awarded M.Sc. and Ph.D. theses under his supervision. His research interests include spin transport characteristics through novel semiconductor quantum dots, nanowires, two dimensional materials (graphene, silicene), quantum transport characteristics of carbon nanotube, and graphene nanoribbons.

AHMED SAEED ABDELRAZEK BAYOUMI was born in Cairo, Egypt, in 1983. He received the B.Sc. degree in electronics and communication engineering and the M.Sc. and Ph.D. degrees from Ain Shams University, Egypt, in 2005, 2013, and 2016, respectively. He is currently an Assistant Professor with the Engineering Physics and Mathematics Department, Faculty of Engineering, Kafrelsheikh University, Egypt. His research interests include spin transport properties in nanostructures and its applications, optimization and PV, and its application.